

Synthesis and reactions of coordinatively unsaturated 16-electron chalcogenolate complexes, $\text{Ru}(\text{EAr})_2(\eta^6\text{-arene})$ and cationic binuclear chalcogenolate complexes, $[(\eta^6\text{-arene})\text{Ru}(\mu\text{-EPh})_3\text{Ru}(\eta^6\text{-arene})]\text{PF}_6$

Kazushi Mashima^{a,*}, Sei-ichi Kaneko^a, Kazuhide Tani^a, Hiromu Kaneyoshi^b,
Akira Nakamura^b

^a Department of Chemistry, Graduate School of Engineering Science, Osaka University, Toyonaka, Osaka 560, Japan

^b Department of Macromolecular Science, Graduate School of Science, Osaka University, Toyonaka, Osaka 560, Japan

Received 19 March 1997; received in revised form 20 June 1997

Abstract

Coordinatively unsaturated 16-electron ruthenium–selenolate complexes $(\eta^6\text{-arene})\text{Ru}(\text{Se-2,4,6-}\text{C}_6\text{H}_2\text{Me}_3)_2$ [arene = *p*- $\text{CH}_3\text{C}_6\text{H}_4(\text{CHMe}_2)$ (**5b**), C_6Me_6 (**5c**)] have been prepared by treating $[(\eta^6\text{-arene})\text{RuCl}_2]_2$ (**1**) with sodium salt of 2,4,6-trimethylphenylselenolate in methanol. The complexes **5** are compared with the thiolate complexes such as $(\eta^6\text{-arene})\text{Ru}(\text{SAr})_2$ [SAr = 2,6-dimethylbenzenethiolate (**2**), SAr = 2,4,6-tri(isopropyl)benzenethiolate (**3**), (SAr)₂ = 1,2-benzenedithiolate (**4**); arene = C_6H_6 (**a**), *p*- $\text{CH}_3\text{C}_6\text{H}_4(\text{CHMe}_2)$ (**b**), C_6Me_6 (**c**)], which have been recently prepared by us. However, the telluroate analog has not been obtained in similar manner. These selenolate complexes are dark green, being ascribed to the LMCT band $[p\pi(\text{Se}) \rightarrow d\pi^*(\text{Ru})]$. The absorption bands of **5** are red-shifted compared to the thiolate complexes. In contrast to the bulky substituted chalcogenolate ligand system, the reaction of **1** with PhENA followed by the addition of KPF_6 resulted in the formation of the cationic binuclear chalcogenolate complexes $[(\eta^6\text{-arene})\text{Ru}(\mu\text{-E-Ph})_3\text{Ru}(\eta^6\text{-arene})](\text{PF}_6)$ [E = Se (**7**), E = Te (**8**); arene = *p*- $\text{CH}_3\text{C}_6\text{H}_4(\text{CHMe}_2)$ (**b**), C_6Me_6 (**c**)]. Reactions of the 16-electron thiolate and selenolate complexes with σ -donor molecules such as DMSO, hydrazine and ammonia along with some electrophiles were investigated. DMSO can coordinate with the thiolate complex **2a** to give a DMSO adduct of **9**, which was characterized spectroscopically and crystallographically. The strength of complexation of hydrazine and ammonia to the thiolate and selenolate complexes **2**, **3**, **4c** and **5** depends on the effective electron deficiency of the ruthenium supported by η^6 -arene ligand and two chalcogenolate ligands. Two new hydrazine complexes $(\eta^6\text{-C}_6\text{H}_6)\text{Ru}(\eta^1\text{-NH}_2\text{NH}_2)(\text{S-2,6-}\text{C}_6\text{H}_3\text{Me}_2)_2$ (**10a**) and $[(\eta^6\text{-C}_6\text{Me}_6)\text{Ru}(\text{S}_2\text{C}_6\text{H}_4)_2](\mu\text{-NH}_2\text{NH}_2)$ (**16**) were crystallographically characterized. The observed two different coordination modes, mononuclear η^1 -hydrazine and binuclear μ -hydrazine, were the results of the combined steric effect of the arene and the thiolate coligands as well as the $\text{NH} \cdots \text{S}$ hydrogen bonding. © 1997 Elsevier Science S.A.

Keywords: Ruthenium; Thiolate; Selenolate; Tellurate; Hydrazine; Crystal structure; Mononuclear; Dinuclear; 16-electron complex

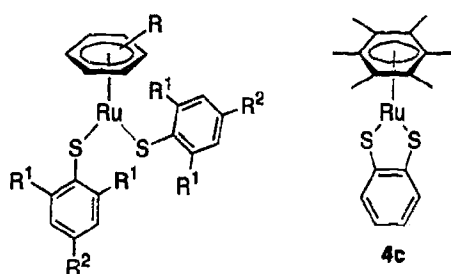
1. Introduction

In a recent paper we reported the synthesis of coordinatively unsaturated 16-electron ruthenium–thiolate complexes of general formula $(\eta^6\text{-arene})\text{Ru}(\text{SAr})_2$ [SAr = 2,6-dimethylbenzenethiolate = SXyl (**2**), SAr = 2,4,6-tri(isopropyl)benzenethiolate (**3**), (SAr)₂ = 1,2-benzenedithiolate (**4**); arene = C_6H_6 (**a**), *p*- $\text{CH}_3\text{C}_6\text{H}_4(\text{CHMe}_2)$ (**b**), C_6Me_6 (**c**)] by treating $[(\eta^6\text{-arene})\text{RuCl}_2]_2$ (**1**) with sodium salts of arenethiolates,

together with their structure and reactions with π -accepting molecules [1,2]. An investigation of the interaction of unsaturated thiolate complexes of group 8 metals with nitrogen-containing molecules such as hydrazine [3–6], diazene [5,7,8] and ammonia [5] has attracted much interest. A change in the chalcogen element from sulfur to selenium should perturb the bonding nature of the 16-electron coordinatively unsaturation on chalcogenolate ruthenium complexes, thereby altering the stability and reactivity of the 16-electron selenolate complexes and allowing us to investigate also the reaction of $(\eta^6\text{-arene})\text{Ru}(\text{SeAr})_2$ with σ -donor

* Corresponding author.

molecules. In this paper we report the preparation and characterization of selenolate complexes of the general formula of $(\eta^6\text{-arene})\text{Ru}(\text{Se-2,4,6-C}_6\text{H}_2\text{Me}_3)_2$ [arene = $p\text{-CH}_3\text{C}_6\text{H}_4(\text{CHMe}_2)$ (**5b**), C_6Me_6 (**5c**)] and reactions of 16-electron chalcogenolate complexes with σ -donor molecules and the crystal structures of the DMSO adduct $(\eta^6\text{-C}_6\text{H}_6)\text{Ru}(\eta^1\text{-OSMe}_2)(\text{S-2,6-C}_6\text{H}_3\text{Me}_2)_2$ (**9**), the mononuclear η^1 -hydrazine complex $(\eta^6\text{-C}_6\text{H}_6)\text{Ru}(\eta^1\text{-NH}_2\text{NH}_2)(\text{S-2,6-C}_6\text{H}_3\text{Me}_2)_2$ (**10a**) and the binuclear μ -hydrazine complex $[(\eta^6\text{-C}_6\text{Me}_6)\text{Ru}(\text{S}_2\text{C}_6\text{H}_4)]_2(\mu\text{-NH}_2\text{NH}_2)$ (**16**) along with the cationic binuclear thiolate and selenolate complexes of ruthenium(II). A part of this work has been the subject of preliminary communications [1,9].



- 2:** $\text{R}^1 = \text{Me}$, $\text{R}^2 = \text{H}$
3: $\text{R}^1 = \text{R}^2 = \text{CHMe}_2$

- a:** arene = C_6H_6
b: arene = $p\text{-cymene}$
c: arene = C_6Me_6

2. Results and discussion

2.1. Mononuclear 16-electron selenolate complexes of ruthenium(II), $(\eta^6\text{-arene})\text{Ru}(\text{SeC}_6\text{H}_2\text{Me}_3\text{-2,4,6})_2$

We prepared the selenolate complexes of the general formula $(\eta^6\text{-arene})\text{Ru}(\text{SeMes})_2$ [$p\text{-CH}_3\text{C}_6\text{H}_4(\text{CHMe}_2)$ (**5b**), C_6Me_6 (**5c**); Mes = 2,4,6-trimethylphenyl] in the same manner as the preparation of thiolate complexes 2–4 [1,2]. Treatment of $[(\eta^6\text{-C}_6\text{Me}_6)\text{RuCl}_2]_2$ (**1c**) with 1.5-fold excess of sodium 2,4,6-trimethylbenzeneselenolate in methanol resulted in the rapid precipitation of $(\eta^6\text{-C}_6\text{Me}_6)\text{Ru}(\text{SeMes})_2$ (**5c**) as dark green microcrystals in 48% yield. Similarly, complex $(\eta^6\text{-}p\text{-cymene})\text{Ru}(\text{SeMes})_2$ (**5b**) was isolated in 63% yield by reaction of $[(\eta^6\text{-}p\text{-cymene})\text{RuCl}_2]_2$ (**1b**) with sodium 2,4,6-trimethylbenzeneselenolate. Efforts to isolate benzene complex $(\eta^6\text{-C}_6\text{H}_6)\text{Ru}(\text{SeMes})_2$ (**5a**) by treating $[(\eta^6\text{-C}_6\text{H}_6)\text{RuCl}_2]_2$ (**1a**) with sodium 2,4,6-trimethylbenzeneselenolate in methanol have been hindered by its high thermal instability. The color of complexes **5b** and **5c** is dark green and their absorption bands (λ_{max} of

Table 1

Comparative data of LMCT band for some coordinatively unsaturated ruthenium–chalcogenolate complexes and the related complexes

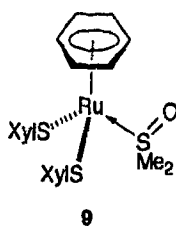
Complex ^a	Color or λ_{max} (nm)	References
$(\eta^4\text{-C}_4\text{Me}_2(\text{tBu})_2)\text{Pd}(1,2\text{-S}_2\text{C}_6\text{H}_4)$	560	[21]
$\text{Cp}^*\text{Ir}(\text{SC}_6\text{F}_5)_2$	deep green	[22]
$\text{Cp}^*\text{Ir}(\text{SC}_6\text{F}_4\text{H-}p)_2$	deep green	[22,23]
2a	698	[2]
2b	676	[1]
2c	660	[2]
3a	715	[2]
3b	686	[1]
3c	669	[2]
4c	563	[2]
5b	728	this work
5c	698	this work
$\text{Cp}^*\text{Ru}(\text{PisoPr}_3)\text{Cl}$	576	[12]
$\text{Cp}^*\text{Ru}(\text{PisoPr}_2\text{Ph})\text{I}$	dark blue	[13]
$[\text{Cp}^*\text{Ru}(\mu\text{-OMe})_2]$	506	[15,16]
$[\text{Cp}^*\text{Ru}(\mu\text{-SEt})_2]$	693	[17]
$[(\eta^6\text{-C}_6\text{H}_6)\text{Ru}(\mu\text{-NC}_6\text{H}_3(\text{isoPr})_2\text{-2,6})_2]$	deep green	[19]
$\text{Ru}(\text{SC}_6\text{F}_5)_2(\text{PPh}_3)_2$	purple	[20]
$(\eta^6\text{-}p\text{-cymene})\text{Os}(\text{S}t\text{Bu})_2$	purple	[24,25]
$(\eta^6\text{-}p\text{-cymene})\text{Os}(\text{SC}_6\text{H}_3\text{Me}_2\text{-2,6})_2$	purple	[25]
$\text{trans-}[\text{Re}(\text{SPh})_2(\text{depe})_2]^+$	purple	[26]
$[\text{Cr}(\text{CO})_3(1,2\text{-S}_2\text{C}_6\text{H}_4)]^{2-}$	507	[27]
$\text{CpMo}(\text{NO})(\text{SPh})_2$	dark green	[28]
$\text{Tp}^*\text{Mo}(\text{O})(\text{SPh})_2$	dark green	[29]

^aAbbreviation: Cp^* = η^5 -pentamethylcyclopentadienyl; Tp^* = tris(3,5-dimethylpyrazolyl)hydroborate; depe = 1,2-bis(diethylphosphino)ethane.

728 nm for **5b** and 698 nm for **5c**) in the electronic spectra are assigned to the LMCT band in which a filled $p\pi$ -orbital of selenium atom donates some electrons to a vacant d-orbital of the ruthenium center; in good accordance with the MO description for 16-electron half-sandwich transition metal complexes [10,11]. These correspond to the LMCT band observed for the coordinatively unsaturated ruthenium(II) complexes such as 2–4 [1,2], $\text{Cp}^*\text{RuCl}[\text{P}(\text{isoPr})_3]$ [12], $\text{Cp}^*\text{Ru}[\text{PPh}(\text{isoPr})_2]$ [13], $[\text{Cp}^*\text{Ru}(\mu\text{-OMe})_2]$ [14–16], $[\text{Cp}^*\text{Ru}(\mu\text{-SR})_2]$ [17,18], $[(\eta^6\text{-C}_6\text{H}_6)\text{Ru}(\mu\text{-NC}_6\text{H}_3(\text{isoPr})_2\text{-2,6})_2]$ [19], $\text{Ru}(\text{SC}_6\text{F}_5)_2(\text{PPh}_3)_2$ [20] and related complexes listed in Table 1. The LMCT bands of **5b** and **5c** are red-shifted compared with the corresponding thiolate complexes **2b** (672 nm), **2c** (660 nm), **3b** (686 nm) and **3c** (669 nm). Similar red-shift was reported for chalcogenolate complexes of nickel $[\text{Ni}(\text{ECH}_2\text{CH}_2)_2\text{NMe}]_2$ (E = S and Se) [30]. Unfortunately, all attempts to prepare the telluroate analog have been in failure due to the liberation of the aromatic ligand bound to the ruthenium.

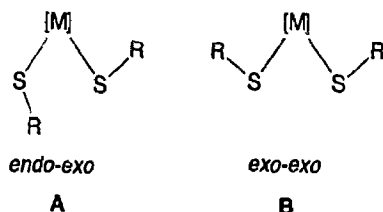
The ^1H NMR spectrum of **5b** in CDCl_3 showed that the ruthenium atom was coordinated by one $\eta^6\text{-}p\text{-cymene}$ ligand and two selenolate ligands with the exact

ditionated to ruthenium atom in the range of 1107–1134 cm^{-1} [35–38], while those of the *O*-coordination in the range of 883–957 cm^{-1} [36,38,39]. Accordingly the *S*-bound structure of **9** is shown below.

**9**

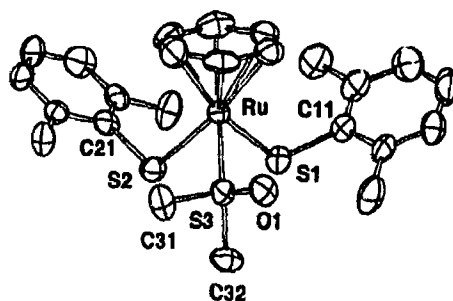
The X-ray molecular structure of the adduct **9** is shown in Fig. 1 where the solvated Me_2SO molecule is omitted for clarity. Selected bond distances and bond angles are shown in Table 2. The ruthenium atom adopts a three-legged piano stool geometry comprised of a η^6 -benzene, two SXyl ligands and an *S*-coordinated dimethyl sulfoxide. The distance (1.702 Å) between the ruthenium and the centroid of the η^6 -benzene ligand of **9** is longer by 0.016 Å than that of **2a**. Geometry around the ruthenium center is closely related to $(\eta^6\text{-C}_6\text{Me}_6)\text{Ru}(\text{9S3})$ (9S3 = 1,4,7-trithiacyclononane) and its deprotonated derivatives [40,41]. The distances of Ru–S(1) and Ru–S(2) (2.439(3) and 2.427(3) Å) are longer than those found for **2a**, **2b**, **3c** and **4c**. The Ru–S(3) (2.331(3) Å) is comparable to those of *S*-coordinated dimethyl sulfoxide complexes of ruthenium reported so far [35,36,38].

With regard to the conformation of two thiolate ligands, the *endo-exo* conformation (**A**) of the starting complex **2a** turned to the *exo-exo* one (**B**) of **9** in order to minimize the steric interaction between the two xylyl ligands and the *S*-coordinated DMSO molecule.

**A****B**

2.4. Reaction of $(\eta^6\text{-arene})\text{Ru}(\text{EAR})_2$ with NH_2NH_2 and NH_3

N-donor molecules such as hydrazine and ammonia coordinated reversibly to the 16-electron coordinatively unsaturated ruthenium(II) thiolate and selenolate complexes. Addition of an excess of $\text{NH}_2\text{NH}_2 \cdot \text{H}_2\text{O}$ to a solution of **2a** in THF induced a rapid change of the solution color from deep blue to deep red; from the concentrated solution a hydrazine complex **10a** was

Fig. 1. ORTEP drawing of **9** with the numbering scheme.

obtained in 70% yield as red-orange crystalline solids. Similar treatment of **2a** with aqueous NH_3 afforded the corresponding complex **11a** in 80% yield. The formulation of these complexes is supported by both of the ^1H NMR spectrum and the elemental analysis. The ^1H NMR spectrum of **10a** displayed a singlet at δ 4.73 due to η^6 -benzene protons and signals due to the SXyl ligands in 1:2 ratio, and in addition a broad singlet around 3.97 ppm due to four protons of the hydrazine moiety. The ^1H NMR spectrum of **11a** displayed a broad singlet at δ 1.11 due to NH_3 and a singlet at δ 4.78 due to one η^6 -benzene ligand together with signals of the two SXyl ligands. The coordination of the hydrazine to the ruthenium in **10a** was supported by its IR spectrum; two $\nu(\text{NH})$ bands at 3300 and 3200 cm^{-1} . The FAB mass spectrum of **10a** showed no parent peak due to **10a**. The release of the hydrazine ligand was also observed for the UV spectrum of **10a** in THF, which exhibited the LMCT band (deep blue color) due to **2a**.

Table 2
Selected bond distances (Å) and angles (deg) of **9**.

Bond distances (Å)	
Ru–S(1)	2.439(3)
Ru–S(2)	2.427(3)
Ru–S(3)	2.331(3)
Ru–CEN	1.702
S(1)–C(11)	1.79(1)
S(2)–C(21)	1.77(1)
S(3)–O(1)	1.488(6)
S(3)–C(31)	1.77(1)
S(3)–C(32)	1.77(1)
Bond angles (deg)	
S(1)–Ru–S(2)	81.6(1)
S(1)–Ru–CEN	128.7
S(2)–Ru–CEN	132.2
S(3)–Ru–CEN	125.9
S(1)–Ru–S(3)	88.7(1)
S(2)–Ru–S(3)	83.9(1)
Ru–S(1)–C(11)	112.7(3)
Ru–S(2)–C(21)	108.5(3)
Ru–S(3)–O(1)	116.1(3)
Ru–S(3)–C(31)	110.7(4)
Ru–S(3)–C(32)	116.3(4)

CEN = the centroid of aromatic ring carbons, C(1)–C(6), of the ligand.

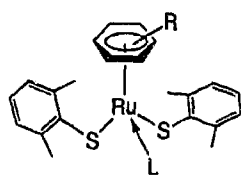
Table 3
Summary for the reaction of **2**, **3** and **5** with hydrazine and ammonia

Complex	NH ₂ NH ₂	NH ₃
2a	10a : isolated	11a : isolated
2b	10b : $K_{eq} = 91.1 \pm 0.6$	11b : $K_{eq} = 3.5 \pm 0.3$
2c	N.R.	N.R.
3a	12a : isolated	13a : isolated
3b	12b : $K_{eq} = 20.7 \pm 3.5$	13b : $K_{eq} = 1.9 \pm 0.7$
3c	N.R.	N.R.
5a	14a : isolated	15a : isolated
5b	14b : isolated	15b : $K_{eq} = 16.6 \pm 3.2$
5c	14c : $K_{eq} = 28.8 \pm 1.0$	15c : $K_{eq} = 4.4 \pm 0.6$

Isolated = the 18-electron adduct was isolated and characterized; N.R. = no reaction; K_{eq} = the equilibrium constant (l mol⁻¹) for the formation of 18-electron adduct in THF solution at 24°C.

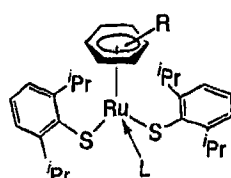
For complex **11a**, we also observed the release of the ammonia ligand, and hence the FAB mass spectrum gave no parent peak due to **11a**.

The stability of *N*-donor adducts depends on the substituent of the η⁶-arene ligand as well as the kind of chalcogens, i.e., sulfur or selenium. In addition to the case of complex **2a**, the complexation of **2**, **3** and **5** with hydrazine and ammonia was investigated. The results are summarized in Table 3. Although **5a** was not isolated as described in Section 2.1, we isolated complexes **14a** and **15a** by the reactions of **2a** with sodium salt of 2,4,6-trimethylbenzeneselenolate in THF in the presence of hydrazine hydrate and ammonia, respectively. Thus, all of the benzene complexes **12a**, **13a**, **14a** and **15a** were isolated and their spectral data are given in Section 4.



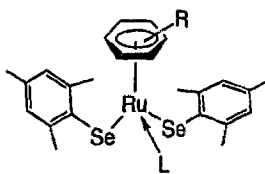
10: L = NH₂NH₂

11: L = NH₃



12: L = NH₂NH₂

13: L = NH₃



14: L = NH₂NH₂

15: L = NH₃

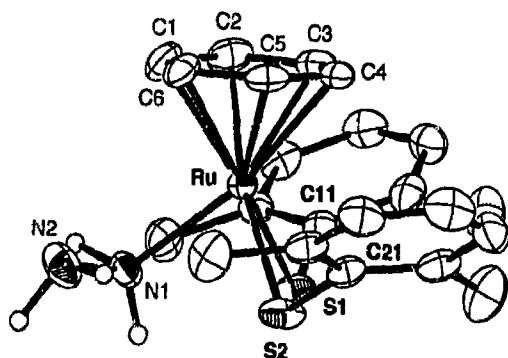
When the *p*-cymene ligand was used, *N*-donor adducts **10b**, **11b**, **12b**, **13b** and **15b** were too labile to be isolated with an exception of **14b** that was obtained in 80% yield. Treatment of **2b** with an excess of

NH₂NH₂ · H₂O in THF induced a rapid change of the color from deep blue to deep orange, yielding an 18-electron hydrazine complex **10b**. After the solution was concentrated under reduced pressure at room temperature, we obtained blue solids of the starting complex **2b**. Consequently, this reaction was in the equilibrium between **2b** and **10b**; the estimated K_{eq} using absorption spectra at 24°C being 91.1 ± 0.6 l mol⁻¹. Similar color change was observed for the reactions of **2b** and **3b** with the *N*-donor molecules and the reaction of **5b** with ammonia, and the K_{eq} values for these equilibrium were estimated by measuring UV spectra at variable concentrations of the *N*-donor molecules. Since the thiolate complexes **2c** and **3c** have the bulky C₆Me₆ ligand, they did not react with the *N*-donor molecules at all. In the case of the selenolate analog **5c**, the *N*-donor molecules were able to coordinate with the ruthenium and K_{eq} values were estimated in similar manner. Thus, the combined effect of electron-donating substituents on the η⁶-benzene ligand and harder chalcogen, which has lateral pπ-orbital suitable to interact with vacant dπ orbital, stabilized the coordinative unsaturation of the ruthenium center and retarded the formation of *N*-donor adducts.

Although both of the nitrogen atoms of the hydrazine have capability to coordinate with the mononuclear ruthenium complex, all hydrazine complexes **10**, **12** and **14** were monomeric. This is attributed to the bulkiness around the ruthenium that prevents the formation of hydrazine-bridged binuclear complex. We expected less bulky mononuclear thiolate complex **4c** to form a binuclear complex. This was successful in our case. Treatment of **4c** with an excess of hydrazine hydrate and the following crystallization from dichloromethane and hexane afforded the hydrazine-bridged binuclear complex [(η⁶-C₆Me₆)Ru(S₂C₆H₄)₂(μ-NH₂NH₂)] (16) as red crystalline solid in 71% yield. The IR spectrum of a solid sample of **16** exhibited bands due to hydrazine coordination with the ruthenium center, though the ¹H NMR spectrum of **16** displayed only signals attributable to **4c** along with signals due to free hydrazine in an exact integral ratio, indicating that the hydrazine was completely liberated in solution.

2.5. Crystal structures of **10a** and **16**

Preliminary structural features of complexes **10a** and **16** were communicated [9]. Two coordination modes, i.e., η¹ or η², are possible for the mononuclear hydrazine complexes, whose structures could not be determined on the basis of these spectral data. The X-ray analysis of **10a** revealed distinctly the mononuclear η¹-coordination mode. Complex **2a** crystallized in rhombohedral space group R3(*h*) and its crystal struc-

Fig. 2. A drawing of **10a** with the atom-labeling scheme.

ture is provided in Fig. 2. Selected bond distances, angles and torsion angles are listed in Table 4.

Complex **10a** adopts the three-legged piano stool geometry where the ruthenium atom is surrounded with η^6 -benzene, two 2,6-XylS and η^1 -hydrazine ligands. The η^1 -coordination mode of hydrazine derivatives has already been found for organoruthenium complexes such as $[\text{Ru}(\eta^1\text{-NH}_2\text{NHR})_3(\text{cod})]^{2+}$ [42] and $[\text{Ru}(\text{H})(\eta^1\text{-NH}_2\text{NMe}_2)_3(\text{cod})]^+$ [43]. The Ru–S bond distances (2.398(3) and 2.419(2) Å) are longer by 0.13 Å than those found for complex **2a** [2] and **2b** [1] in good accordance with the diminution of donative $\text{S}(\text{p}\pi) \rightarrow \text{Ru}(\text{d}\pi^*)$ interaction by the coordination of the nitrogen of hydrazine. The Ru–N bond distance (2.143(7) Å) is comparable to those found for ammine and amine complexes such as $[\text{CpRu}(\text{NH}_3)(\text{PPh}_3)_2]^+$ (2.172(3) Å) [44] and $[\text{CpRu}(\text{NH}_2\text{C}_8\text{H}_{17-1})(\text{Cy}_2\text{PCH}_2\text{CH}_2\text{PCy}_2)]^+$ (2.174(8) Å) [44]. The coordination of hydrazine changed the conformation of the two thiolate ligands; an *endo-exo* conformation in **2a** turned to an *exo-exo* one in **10a**, similar to the case of the formation of DMSO adduct **9**.

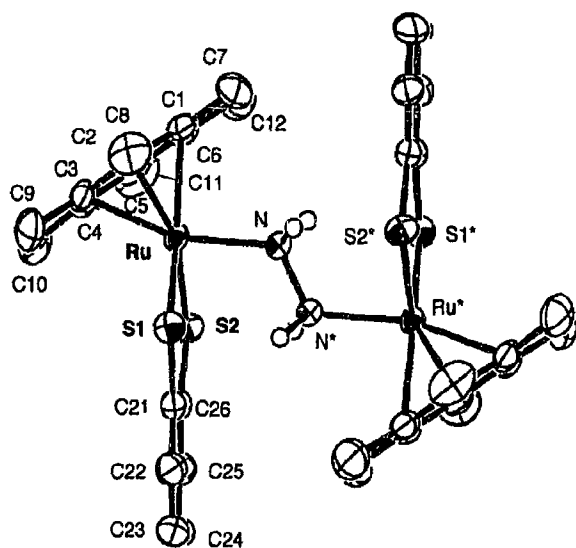
Fig. 3. A drawing of **16** with the labeling scheme.

Table 4

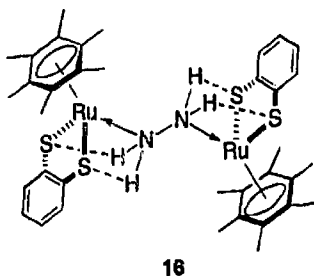
Selected bond distances (Å), angles (deg) and torsion angles (deg) for **10a**

Bond distances (Å)	
Ru–S(1)	2.419(2)
Ru–S(2)	2.398(3)
Ru–C(1)	2.150(9)
Ru–C(2)	2.201(9)
Ru–C(3)	2.179(9)
Ru–C(4)	2.194(9)
Ru–C(5)	2.198(9)
Ru–C(6)	2.194(9)
Ru–CEN	1.675
S(1)–C(11)	1.777(9)
S(2)–C(21)	1.759(10)
Ru–N(1)	2.143(7)
N(1)–N(2)	1.378(10)
Bond angles (deg)	
Ru–S(1)–C(11)	110.0(3)
Ru–S(2)–C(21)	109.7(3)
S(1)–Ru–S(2)	82.24(9)
S(1)–Ru–CEN	131.8
S(2)–Ru–CEN	133.0
N(1)–Ru–CEN	127.6
N(2)–N(1)–Ru	117.9(6)
Torsion angles (deg)	
S(2)–Ru–S(1)–C(11)	–161.3(3)
CEN–Ru–S(1)–C(11)	–18.0
S(1)–Ru–S(2)–C(21)	130.6(4)
CEN–Ru–S(2)–C(21)	–12.0
S(1)–Ru–N(1)–N(2)	164.0(7)
S(2)–Ru–N(1)–N(2)	80.6(7)

CEN = the centroid of aromatic ring carbons, C(1)–C(6), of the ligand.

The crystal of **16** belongs to the monoclinic space group $C2/c$ with four binuclear molecules that have a C_2 axis passing through the center of the N–N bond of the bridging hydrazine ligand. Fig. 3 shows the crystal structure of **16**. Selected bond distances and angles are listed in Table 5. Each ruthenium center in complex **16** adopts a three-legged piano stool geometry that has unexceptional bond distances and angles around the ruthenium atom. The N–N bond distance (1.454(8) Å) of **16** is normal as expected for the μ -hydrazine binuclear complexes such as $\{\text{RuCl}(\text{P}(\text{OMe})_3)_2\}_2(\mu\text{-S}_2)(\mu\text{-Cl})(\mu\text{-N}_2\text{H}_4)$ (1.442(1) Å) [3], $[\{\text{Ru}(\text{acetonitrile})(\text{P}(\text{OMe})_3)_2\}_2(\mu\text{-S}_2)(\mu\text{-N}_2\text{H}_4)_2]^{3+}$ (1.465(14) and 1.477(13) Å) [4], $[\text{W}(\text{NPh})\text{Me}_3]_2(\mu\text{-}\eta^1, \eta^1\text{-NH}_2\text{NH}_2)(\mu\text{-}\eta^2, \eta^2\text{-NHNH})$ (1.434(14) Å) [45] and $[\{\text{MoO}(\text{S}_2)_2\}_2(\mu\text{-S}_7)(\mu^2\text{-NH}_2\text{NH}_2)]^{2-}$ (1.40(1) Å) [46], but is much longer than that (1.378(10) Å) of **10a**, because the σ -donation of lone pair electrons on a nitrogen atom of hydrazine was enforced by further σ -donative interaction of lone pair electrons of the neighboring nitrogen atom of hydrazine. In the complex **16**, the hydrazine may function as a bridging ligand through the $\text{NH} \cdots \text{S}$ hydrogen bonds (3.18 and 3.22

Å), values which are within the range of $\text{NH}\cdots\text{S}$ hydrogen bonding observed for $[\text{Me}_2\text{NHCH}_2\text{CH}_2\text{NHMe}_2][\text{Pd}(\text{SC}_6\text{F}_5)_4]$ (3.256(6) Å) [47], $[\text{Me}_3\text{NCH}_2\text{CONH}_2]_2[\text{Co}(\text{SPh})_4]$ (3.316(3)–3.453(3) Å) [48], (tris(3,5-dimethylpyrazolyl)-hydroborate) $\text{Mo}(\text{NO})(\text{SCH}_2\text{CONHCH}_3)_2$ (2.971(4) Å) [49] and $[\text{Mo}(\text{O})(\text{S}-o\text{-CH}_3\text{CONH}-\text{C}_6\text{H}_4)_4]^-$ (2.97–3.03 Å) [50].



16

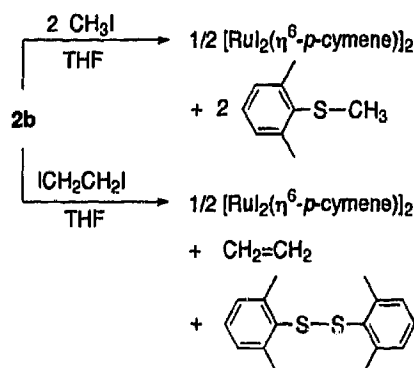
2.6. Reactions with MeI and 1,2-diiodoethane

In order to assess the nucleophilic nature of the thiolate ligand bound to ruthenium, we examined the

Table 5
Selected bond distances (Å), angles (deg) and torsion angles (deg) for 16

Bond distances (Å)	
Ru–S(1)	2.370(2)
Ru–S(2)	2.364(1)
Ru–C(1)	2.217(5)
Ru–C(2)	2.211(5)
Ru–C(3)	2.217(5)
Ru–C(4)	2.200(5)
Ru–C(5)	2.213(5)
Ru–C(6)	2.220(6)
Ru–CEN	1.692
S(1)–C(21)	1.766(5)
S(2)–C(26)	1.752(5)
Ru–N(1)	2.147(4)
N(1)–N(1)*	1.454(8)
Bond angles (deg)	
Ru–S(1)–C(21)	106.0(2)
Ru–S(2)–C(26)	105.9(2)
S(1)–Ru–S(2)	85.87(5)
S(1)–Ru–CEN	129.0
S(2)–Ru–CEN	125.2
N(1)–Ru–CEN	121.5
N(1)*–N(1)–Ru	120.8(4)
Torsion angles (deg)	
S(2)–Ru–S(1)–C(21)	–1.3(2)
CEN–Ru–S(1)–C(21)	136.5.0
S(1)–Ru–S(2)–C(26)	2.3(2)
CEN–Ru–S(2)–C(26)	–138.0
S(1)–Ru–N(1)–N(1)*	42.3(5)
S(2)–Ru–N(1)–N(1)*	–43.8(5)

CEN = the centroid of aromatic ring carbons, C(1)–C(6), of the ligand.



Scheme 1.

reaction of **2b** with electrophiles such as iodomethane and 1,2-diiodoethane. The reaction of **2b** with an excess of iodomethane in CDCl_3 produced $[(\eta^6\text{-}p\text{-cymene})\text{Ru}]_2$ (**17**) and 2,6-dimethylphenyl methyl thioether, as monitored by the ^1H NMR spectrum (Scheme 1). Methylation of the thiolate ligand bound to the ruthenium has been known to result in the formation of cationic thioether complexes [51–53]. Treatment of **2b** with 1,2-diiodoethane resulted in the formation of **17**, ethylene and dityl disulfide (detected by ^1H NMR). The formation of disulfide might be related to the reported example in which the one-electron oxidation of $\text{CpM}(\text{PR}_3)(\text{L})(\text{SR}')^+$ ($\text{M} = \text{Fe}, \text{Ru}; \text{L} = \text{PR}_3, \text{CO}$) produced the corresponding disulfide complex $[(\text{CpM}(\text{PR}_3)(\text{L}))_2(\mu\text{-S}_2\text{R}')^2]^+$ [54–56].

3. Conclusion

Our current investigation on the 16-electron coordinatively unsaturated chalcogenolate complexes of ruthenium(II) has shown that $d\pi\text{-}p\pi$ interaction between the metal and the chalcogen considerably weakens the electron deficiency at the ruthenium. Steric-congested coordination site also affects their behavior for addition of donors, and therefore small σ -type donors are preferred. However, typical small σ -donors exemplified by ammonia and hydrazine did not strongly coordinate to the ruthenium. A combined effect of steric and electronic characteristics thus determines the observed chemical properties of this class of complexes.

4. Experimental section

4.1. General

All manipulations involving air- and moisture-sensitive organometallic compounds were carried out by the use of the standard Schlenk technique under argon atmosphere. Dichloromethane was purified by distillation under argon after drying over calcium hydride.

Methanol was dried over magnesium alkoxide. THF, toluene and hexane were dried over sodium benzo-phenone ketyl and then distilled before use. Complexes $[\text{RuCl}_2(\eta^6\text{-arene})_2]$ (**1**) [57] and thiolate complexes **2–4** [2] were prepared according to the literature methods. Dimesityl diselenide [58] and diphenyl ditelluride [59] were prepared according to the literature procedures.

Nuclear magnetic resonance [^1H (400 MHz and 270 MHz) and ^{31}P (36 MHz) NMR] spectra were measured on a JEOL JNM-GX400, JEOL JNM-GSX-270 and JEOL EX-270 spectrometers. All ^1H NMR chemical shifts were reported in ppm relative to protio impurity resonance as follows: chloroform-*d*, singlet at 7.27 ppm; benzene-*d*₆, singlet at 7.20 ppm and ^{31}P NMR chemical shifts were reported in ppm relative to external reference of 85% H_3PO_4 at 0.00 ppm. Other spectra were recorded by the use of the following instruments: IR, Hitachi 295; mass spectra, JEOL SX-102 spectrometer operating in the FAB+ mode by using 3-nitrobenzyl alcohol (N.B.A.) as a matrix; UV/vis spectra, Jasco Ubest-30 and Shimadzu UV-265FS. Elemental analyses were performed at the Elemental Analysis Center, Osaka University. All melting points were measured in sealed tubes and were not corrected.

4.2. Preparation of $\text{Ru}(\eta^6\text{-}p\text{-cymene})(\text{SeC}_6\text{H}_2\text{Me}_3\text{-2,4,6})_2$ (**5b**)

To a solution of sodium mesitylselenolate derived from dimesityl diselenide (159 mg, 0.29 mmol) and sodium (29 mg, 1.26 mmol) in methanol (10 ml) was added **1b** (85 mg, 0.14 mmol) at room temperature. The color of the reaction mixture turned rapidly from reddish brown to deep green. After stirring the resulting mixture for 1 h, the dark green precipitate was filtered off, washed with methanol, and then dried in vacuo (110 mg, 63% yield), mp 140–143°C (dec.). ^1H NMR (CDCl_3 , 35°C): δ 1.25 (d, $J = 6.93$ Hz, 6H, $\text{CH}(\text{CH}_3)_2$ of *p*-cymene), 1.81 (s, 3H, *Me* of *p*-cymene), 2.2 (m, CHMe_2), 2.29 (s, 6H, *p*-*Me* of $\text{SeC}_6\text{H}_2\text{Me}_3\text{-2,4,6}$), 2.39 (s, 12H, *o*-*Me* of $\text{SeC}_6\text{H}_2\text{Me}_3\text{-2,4,6}$), 4.81 and 4.95 (AA'BB', $J = 6.0$ Hz, 4H, aromatic protons of *p*-cymene), 6.96 (s, 4H, $\text{SeC}_6\text{H}_2\text{Me}_3\text{-2,4,6}$); FAB MS (N.B.A. matrix): m/z 433 ($\text{M}^+ - \text{SeC}_6\text{H}_2\text{Me}_3\text{-2,4,6}$); UV/vis (THF): λ_{max} 728 nm ($\epsilon = 4.5 \times 10^3 \text{ M}^{-1} \text{ cm}^{-1}$).

4.3. Preparation of $\text{Ru}(\eta^6\text{-}C_6\text{Me}_6)(\text{SeC}_6\text{H}_2\text{Me}_3\text{-2,4,6})_2$ (**5c**)

Complex **1c** (70 mg, 0.11 mmol) was added to a solution of sodium mesitylselenolate derived from dimesityl diselenide (126 mg, 0.23 mmol) and sodium (15 mg, 0.65 mmol) in methanol (8 ml) at room temperature. The color of the reaction mixture changed immediately from reddish brown to deep green. After stirring

the resulting mixture for 1 h, the dark green precipitate (66 mg, 48% yield) was filtered off, washed with methanol, and then dried in vacuo, mp 205–208°C (dec.). ^1H NMR (CDCl_3 , 35°C): δ 1.88 (s, 18H, C_6Me_6), 2.22 (s, 18H, $\text{SeC}_6\text{H}_2\text{Me}_3\text{-2,4,6}$), 6.84 (s, 4H, $\text{SeC}_6\text{H}_2\text{Me}_3\text{-2,4,6}$); FAB MS (N.B.A. matrix): m/z 660 (M^+). UV/vis (THF): λ_{max} 698 nm ($\epsilon = 2.3 \times 10^3 \text{ M}^{-1} \text{ cm}^{-1}$).

4.4. Synthesis of $[(\eta^6\text{-}p\text{-cymene})\text{Ru}(\mu\text{-SePh})_3\text{Ru}(\eta^6\text{-}p\text{-cymene})]\text{PF}_6$ (**7b**)

$[\text{RuCl}_2(\eta^6\text{-}p\text{-cymene})_2]$ (**1b**) (153 mg, 0.25 mmol) was added to a solution of sodium benzeneselenolate, which was prepared from diphenyl diselenide (149 mg, 0.48 mmol) and sodium borohydride (20 mg, 0.53 mmol) in methanol (8 ml) at room temperature. The reaction mixture was stirred overnight and the color turned to brownish black. After being stirred for 3 h, KPF_6 (78 mg, 0.42 mmol) was added to the extracted solution and then the solution was stirred overnight. Precipitates were filtered off and the filtrate was concentrated under reduced pressure. Recrystallization of the residue from dichloromethane and diethyl ether afforded **7b** as deep red microcrystals (51 mg, 19% yield), mp 178–185°C (dec.). ^1H NMR (CDCl_3 , 35°C): δ 0.76 and 0.88 (d, $J = 6.93$ Hz, 12H, CHMe_2 of *p*-cymene), 1.72 (s, 6H, *Me* of *p*-cymene), 2.12 (m, 2H, $\text{CH}(\text{CH}_3)_2$ of *p*-cymene), 5.15 and 5.32 (AA'BB', $J = 5.94$ Hz, 4H, aromatic protons of *p*-cymene), 5.25 and 5.46 (AA'BB', $J = 5.94$ Hz, 4H, aromatic protons of *p*-cymene), 7.3–7.8 (m, 15H, SeC_6H_5); $^{31}\text{P}\{^1\text{H}\}$ NMR (CDCl_3 , 35°C): δ -143.4 (m); FAB MS (N.B.A. matrix): m/z 941 ($\text{M}^+ - \text{PF}_6$); UV/vis (CH_2Cl_2): λ_{max} 328 nm ($\epsilon = 1.0 \times 10^4 \text{ M}^{-1} \text{ cm}^{-1}$).

4.5. Synthesis of $[(\eta^6\text{-}C_6\text{Me}_6)\text{Ru}(\mu\text{-SePh})_3\text{Ru}(\eta^6\text{-}C_6\text{Me}_6)]\text{PF}_6$ (**7c**)

$[\text{RuCl}_2(\eta^6\text{-}C_6\text{Me}_6)_2]$ (**1c**) (90 mg, 0.14 mmol) was added to a solution of sodium benzeneselenolate, which was prepared by the treatment of diphenyl diselenide (77 mg, 0.25 mmol) with sodium borohydride (10 mg, 0.26 mmol) in methanol (7 ml) at room temperature. The reaction mixture was stirred overnight and the color turned to brownish black. After being stirred for 9 h, KPF_6 (55 mg, 0.30 mmol) was added to the extracted solution and then the solution was stirred overnight. White precipitates suspended during the reaction were filtered off and then the filtrate was concentrated under reduced pressure. Recrystallization of the resulting solid from dichloromethane and diethyl ether afforded **7c** as reddish orange crystals (41 mg, 53% yield), mp > 300°C. ^1H NMR (CDCl_3 , 35°C): δ 1.70 (s, 18H, C_6Me_6), 7.2–7.8 (m, 15H, SeC_6H_5); $^{31}\text{P}\{^1\text{H}\}$ NMR (CDCl_3 , 35°C): δ -143.7 (m); FAB MS (N.B.A.

matrix): m/z 995 (M^+ -PF₆); UV/vis (CH₂Cl₂): λ_{\max} 330 nm ($\epsilon = 1.1 \times 10^4$ M⁻¹ cm⁻¹).

4.6. Synthesis of $[(\eta^6\text{-}p\text{-cymene})\text{Ru}(\text{TePh})_3\text{Ru}(\eta^6\text{-}p\text{-cymene})]\text{PF}_6$ (**8b**)

Complex **1b** (79 mg, 0.13 mmol) was added to a solution of sodium benzenetelluroate, which was prepared by the treatment of diphenyl ditelluride (132 mg, 0.32 mmol) with sodium borohydride (14 mg, 0.37 mmol) in methanol (7 ml) at room temperature. The reaction mixture was stirred overnight and the color turned to brownish black. After being stirred for 2 h, KPF₆ (31 mg, 0.17 mmol) was added to the extracted solution and then the solution was stirred overnight. White precipitates suspended during the reaction were filtered off and the filtrate was concentrated under reduced pressure and recrystallization from dichloromethane and diethyl ether afforded **8b** as dark red microcrystals (74 mg, 47% yield), mp 140–149°C (dec.). ¹H NMR (CDCl₃, 35°C): δ 0.78 (d, $J = 6.92$ Hz, 6H, CH(CH₃)₂ of *p*-cymene), 0.89 (d, $J = 6.93$ Hz, 6H, CH(CH₃)₂ of *p*-cymene), 1.95 (s, 6H, Me of *p*-cymene), 2.33 (m, 2H, CH(CH₃)₂ of *p*-cymene), 5.4–5.7 (m, 8H, aromatic protons of *p*-cymene), 7.2–7.7 (m, 15H, TeC₆H₅); ³¹P{¹H} NMR (CDCl₃, 35°C): δ -149.9 (m); FAB MS (N.B.A. matrix): m/z 1084 (M^+ -PF₆); UV/vis (CH₂Cl₂): λ_{\max} 326 nm ($\epsilon = 1.4 \times 10^4$ M⁻¹ cm⁻¹). Anal. calc. for C₄₀H₄₇Cl₄F₆PRu₂Te₃: C, 34.32; H, 3.38. Found: C, 34.72; H, 3.74.

4.7. Synthesis of **9**

Treatment of **2a** (0.10 g, 0.23 mmol) in THF (25 ml) with an excess of Me₂SO (0.24 ml, 3.38 mmol) at room temperature and the following recrystallization from THF (1 ml) and hexane (2 ml) gave **9** as dark purple needles (90 mg, 68% yield), mp 69–71°C (dec.). The ¹H NMR spectrum (CDCl₃, 30°C) showed signals assignable to **2a** and a singlet at δ 2.62 due to two moles of dimethyl sulfoxide. IR (Nujol): $\nu(\text{SO})$: 1040s, 1020s cm⁻¹. Anal. calc. for C₂₆H₃₆O₂RuS₄: C, 51.20; H, 5.95. Found: C, 50.66; H, 5.91.

4.8. Synthesis of $\text{Ru}(\eta^6\text{-}C_6H_6)(\text{SXyl})_2(\eta^1\text{-NH}_2\text{NH}_2)$ (**10a**)

To a solution of $\text{Ru}(\eta^6\text{-}C_6H_6)(\text{SXyl})_2$ (0.26 g, 0.58 mmol) in THF (20 ml) was added an excess of NH₂NH₂ · H₂O (0.28 ml, 5.76 mmol) at room temperature. The color of the solution rapidly turned to dark reddish brown. When all volatiles were removed under reduced pressure, reddish orange microcrystals were precipitated. Recrystallization of this precipitation from a 1:1 mixture of THF and hexane at -20°C afforded **10a** as red crystals (202 mg, 70% yield), mp 138–140°C (dec.). ¹H NMR (CDCl₃, 30°C): δ 2.51 (s, 12H, 2,6-

SC₆H₃Me₂), 3.97 (br, 4H, N₂H₄), 4.73 (s, 6H, C₆H₆), 7.01–7.15 (m, 6H, 2,6-SC₆H₃Me₂); IR (Nujol): $\nu(\text{NH})$: 3300s, 3200m cm⁻¹. Anal. calc. for C₂₂H₂₈N₂RuS₂: C, 54.40; H, 5.81; N, 5.77. Found: C, 54.20; H, 6.07; N, 5.95.

4.9. Synthesis of $\text{Ru}(\eta^6\text{-}C_6H_6)(\text{SXyl})_2(\eta^1\text{-NH}_3)$ (**11a**)

Addition of 2.4 M aqueous NH₃ solution of THF (2.1 ml, 5.08 mmol) to a solution of **2a** (0.22 g, 0.49 mmol) in THF (20 ml) at room temperature induced the change of the color of the solution to dark reddish brown. The solution was concentrated to ca. 10 ml under reduced pressure, and then an additional 2.4 M NH₃ solution of THF (1.5 ml, 3.63 mmol) was added. Hexane (12 ml) was layered to this solution, and was stored at -20°C overnight, affording **11a** as brown needles (185 mg, 80% yield), mp 104–106°C (dec.). ¹H NMR (CDCl₃, 30°C): δ 1.11 (br, 3H, NH₃), 2.47 (s, 12H, 2,6-SC₆H₃Me₂), 4.78 (s, 6H, C₆H₆), 7.01–7.15 (m, 6H, 2,6-SC₆H₃Me₂); IR (Nujol): $\nu(\text{NH})$: 3300s, 3200s, 3120m cm⁻¹. Anal. calc. for C₂₂H₂₇NRuS₂: C, 56.13; H, 5.78; N, 2.98. Found: C, 56.04; H, 5.74; N, 2.96.

4.10. Synthesis of $\text{Ru}(\eta^6\text{-}C_6H_6)(\text{SC}_6\text{H}_2(\text{isoPr})_3\text{-}2,4,6)_2(\eta^1\text{-NH}_2\text{NH}_2)$ (**12a**)

To a solution of **3a** (144 mg, 0.22 mmol) in THF (12 ml) was added an excess of NH₂NH₂ · H₂O (0.14 ml, 2.88 mmol) at room temperature. The color of the solution rapidly turned to deep red. After stirring the resulting mixture for overnight, all volatiles were removed under reduced pressure and recrystallization from a mixture of THF and hexane at -20°C afforded **12a** as dark red microcrystals (121 mg, 80% yield), mp 107–111°C (dec.). ¹H NMR (CDCl₃, 35°C): δ 1.2–1.3 (m, 36H, CHMe₂ of SC₆H₂(isoPr)₃-2,4,6), 2.88 (m, 2H, *p*-CH(CH₃)₂ of SC₆H₂(isoPr)₃-2,4,6), 3.60 (broad, 4H, NH₂NH₂), 3.95 (m, 4H, *o*-CH(CH₃)₂ of SC₆H₂(isoPr)₃-2,4,6), 4.59 (s, 6H, C₆H₆), 7.00 (s, 4H, SC₆H₂(isoPr)₃-2,4,6); FAB MS (N.B.A. matrix): m/z 413 (M^+ -SC₆H₂(isoPr)₃-2,4,6 - NH₂NH₂); IR (Nujol): $\nu(\text{NH})$: 3270w, 3200w, 3190w cm⁻¹. Anal. calc. for C₃₆H₅₆N₂RuS₂: C, 63.39; H, 8.27. Found: C, 63.60; H, 8.22.

4.11. Synthesis of $\text{Ru}(\eta^6\text{-}C_6H_6)(\text{SC}_6\text{H}_2(\text{isoPr})_3\text{-}2,4,6)_2(\eta^1\text{-NH}_3)$ (**13a**)

To a solution of **3a** (58 mg, 0.089 mmol) in THF (2 ml) was added an excess of 2.4 M NH₃ solution of THF (0.2 ml, 0.48 mmol) at room temperature. The color of the solution rapidly turned to deep red. After stirring the resulting mixture for overnight, all volatiles were evaporated under reduced pressure and recrystallization from THF and hexane at -20°C afforded **13a** as reddish

orange needles (28 mg, 47% yield), mp 118–121°C (dec.). $^1\text{H NMR}$ (CDCl_3 , 35°C): δ 1.2–1.3 (m, 36H, CHMe_2 of $\text{SC}_6\text{H}_2(\text{isoPr})_3$ -2,4,6), 1.2 (broad, 3H, NH_3), 2.88 (m, 2H, $p\text{-CH}(\text{CH}_3)_2$ of $\text{SC}_6\text{H}_2(\text{isoPr})_3$ -2,4,6), 3.85 (m, 4H, $o\text{-CH}(\text{CH}_3)_2$ of $\text{SC}_6\text{H}_2(\text{isoPr})_3$ -2,4,6), 4.59 (s, 6H, C_6H_6), 7.00 (s, 4H, $\text{SC}_6\text{H}_2(\text{isoPr})_3$ -2,4,6); FAB MS (N.B.A. matrix): m/z 668 (M^+); anal. calc. for $\text{C}_{36}\text{H}_{55}\text{NRuS}_2$: C, 64.81; H, 8.31. Found: C, 62.00; H, 8.22.

4.12. Synthesis of $\text{Ru}(\eta^6\text{-C}_6\text{H}_6)(\text{SeC}_6\text{H}_2\text{Me}_3\text{-2,4,6})_2(\eta^1\text{-NH}_2\text{NH}_2)$ (**14a**)

Complex **1a** (84 mg, 0.168 mmol) was added to a solution of $\text{NH}_2\text{NH}_2 \cdot \text{H}_2\text{O}$ (0.12 ml, 3.84 mmol) and sodium mesitylselenolate derived from dimesityl diselenide (178 mg, 0.320 mmol) and sodium (13 mg, 0.565 mmol) in THF (5 ml) at room temperature. The color of the reaction mixture immediately turned to reddish brown. After removal of all volatiles under reduced pressure, recrystallization of the residue from dichloromethane and hexane at -20°C afforded **14a** as red microcrystals (130 mg, 64% yield), mp 138–147°C (dec.). $^1\text{H NMR}$ (CDCl_3 , 35°C): δ 2.28 (s, 6H, $p\text{-Me}$ of $\text{SeC}_6\text{H}_2\text{Me}_3$ -2,4,6), 2.51 (s, 12H, $o\text{-Me}$ of $\text{SeC}_6\text{H}_2\text{Me}_3$ -2,4,6), 4.5 (broad, 4H, NH_2NH_2), 4.76 (s, 6H, C_6H_6), 6.96 (s, 4H, $\text{SeC}_6\text{H}_2\text{Me}_3$ -2,4,6); FAB MS (N.B.A. matrix): m/z 376 (M^+ - $\text{SeC}_6\text{H}_2\text{Me}_3$ -2,4,6 - NH_2NH_2); IR (Nujol): $\nu(\text{NH})$: 3447w cm^{-1} .

4.13. Synthesis of $\text{Ru}(\eta^6\text{-}p\text{-cymene})(\text{SeC}_6\text{H}_2\text{Me}_3\text{-2,4,6})_2(\eta^1\text{-NH}_2\text{NH}_2)$ (**14b**)

To a solution of **5b** (61 mg, 0.097 mmol) in THF (3 ml) was added an excess of $\text{NH}_2\text{NH}_2 \cdot \text{H}_2\text{O}$ (0.2 ml, 4.11 mmol) at room temperature. The color of the solution rapidly turned to reddish brown. All volatiles were evaporated and then recrystallized from a mixture of dichloromethane and hexane at -20°C afforded **14b** as deep red microcrystals (51 mg, 80% yield), mp 110–115°C (dec.). $^1\text{H NMR}$ (CDCl_3 , 35°C): δ 1.23 (d, $J = 6.92$ Hz, 6H, $\text{CH}(\text{CH}_3)_2$ of $p\text{-cymene}$), 1.88 (s, 3H, Me of $p\text{-cymene}$), 2.27 (s, 6H, $p\text{-Me}$ of $\text{SeC}_6\text{H}_2\text{Me}_3$ -2,4,6), 2.45 (s, 12H, $o\text{-Me}$ of $\text{SeC}_6\text{H}_2\text{Me}_3$ -2,4,6), 3.34 (broad, 4H, NH_2NH_2), 4.71 and 4.92 (AA'BB', $J = 5.7$ Hz, 4H, aromatic protons of $p\text{-cymene}$), 6.94 (s, 4H, $\text{SeC}_6\text{H}_2\text{Me}_3$ -2,4,6); FAB MS (N.B.A. matrix): m/z 433 (M^+ - $\text{SeC}_6\text{H}_2\text{Me}_3$ -2,4,6 - NH_2NH_2); IR (Nujol): $\nu(\text{NH})$: 3283w, 3222w, 3133w cm^{-1} .

4.14. Synthesis of $\text{Ru}(\eta^6\text{-C}_6\text{H}_6)(\text{SeC}_6\text{H}_2\text{Me}_3\text{-2,4,6})_2(\eta^1\text{-NH}_3)$ (**15a**)

Complex **1a** (75 mg, 0.15 mmol) was added to a 2.4 M solution of NH_3 in THF (0.2 ml, 0.48 mmol) and

sodium mesitylselenolate derived from dimesityl diselenide (192 mg, 0.35 mmol) and sodium borohydride (52 mg, 1.37 mmol) in ethanol (10 ml) at room temperature. All volatiles were removed under reduced pressure and recrystallization from a mixture of dichloromethane and hexane at -20°C afforded **15a** as red microcrystals (66 mg, 57% yield), mp 91–96°C (dec.). $^1\text{H NMR}$ (CDCl_3 , 35°C): δ 1.12 (broad, 3H, NH_3), 2.29 (s, 6H, $p\text{-Me}$ of $\text{SeC}_6\text{H}_2\text{Me}_3$ -2,4,6), 2.46 (s, 12H, $o\text{-Me}$ of $\text{SeC}_6\text{H}_2\text{Me}_3$ -2,4,6), 4.82 (s, 6H, C_6H_6), 6.97 (s, 4H, $\text{SeC}_6\text{H}_2\text{Me}_3$ -2,4,6); FAB MS (N.B.A. matrix): m/z 376 (M^+ - $\text{SeC}_6\text{H}_2\text{Me}_3$ -2,4,6 - NH_2NH_2); IR (Nujol): $\nu(\text{NH})$: 3299w, 3206w cm^{-1} .

4.15. Synthesis of $[\text{Ru}(\eta^6\text{-C}_6\text{Me}_6)(\text{bdt})]_2(\mu\text{-NH}_2\text{NH}_2)$ (**16**)

To a solution of $\text{Ru}(\eta^6\text{-C}_6\text{Me}_6)(\text{S}_2\text{C}_6\text{H}_4)$ (**4c**) (69 mg, 0.17 mmol) in THF (15 ml) was added an excess of $\text{NH}_2\text{NH}_2 \cdot \text{H}_2\text{O}$ (0.10 ml, 2.1 mmol) at room temperature. This solution was stirred overnight, and then all volatiles were removed under reduced pressure. Recrystallization from a 1:1 mixture of dichloromethane and hexane at -20°C afforded **16** as red crystals (51 mg, 71% yield), mp 128–130°C (dec.). $^1\text{H NMR}$ (CDCl_3 , 30°C): δ 2.37 (s, 36H, C_6Me_6), 3.09 (br, 4H, NH_2NH_2), 7.05 and 7.91 (AA'BB' pattern, $^3J = 6.1$ Hz, $^4J = 3.2$ Hz, 8H, 1,2- $\text{S}_2\text{C}_6\text{H}_4$); IR (Nujol): $\nu(\text{NH})$: 3160m, 3080m cm^{-1} . Anal. calc. for $\text{C}_{36}\text{H}_{48}\text{N}_2\text{Ru}_2\text{S}_4(\text{CH}_2\text{Cl}_2)_{0.25}$: C, 50.59; H, 5.68; N, 3.26. Found: C, 50.54; H, 5.73; N, 4.10.

4.16. Reaction of **2b** with *Mel*

To a solution of **2b** (0.18 g, 0.36 mmol) in THF (30 ml) was added an excess of CH_3I (0.40 ml, 6.43 mmol) at room temperature. After the reaction mixture was stirred overnight, the color of the solution turned to dark reddish brown. All volatiles were removed under reduced pressure and the resulting residue was dissolved in THF (5 ml). Recrystallization from a mixture of THF (5 ml) and hexane (3 ml) at 0°C afforded $[\text{RuI}_2(\eta^6\text{-}p\text{-cymene})]_2$ (**17**) as dark brown crystals (55 mg, 31% yield). The $^1\text{H NMR}$ spectrum is superimposed with that of literature [60]. Anal. calc. for $\text{C}_{20}\text{H}_{28}\text{I}_4\text{Ru}_2$: C, 24.56; H, 2.89. Found: C, 24.56; H, 2.85.

4.17. Reaction of **2b** with $\text{ICH}_2\text{CH}_2\text{I}$

To a solution of **2b** (0.13 g, 0.25 mmol) in THF (39 ml) was added an excess of $\text{ICH}_2\text{CH}_2\text{I}$ (0.56 g, 2.00 mmol) at room temperature. After the reaction mixture was stirred overnight, the color of the solution turned to dark reddish brown. All volatiles were removed under reduced pressure and the resulting residue was crystallized from a mixture of THF (5 ml) and hexane (2 ml) at 0°C to give **17** as dark brown crystals (71 mg, 58%).

4.18. Crystallographic studies for complexes **9**, **10a** and **16**

4.18.1. Data collection

Each suitable crystal was mounted in glass capillaries under argon atmosphere. Data for three complexes were collected by a Rigaku AFC-7R diffractometer with a graphite monochromated Mo-K α radiation. Cell constants and an orientation matrix for data collection, obtained from a least-squares refinement using the setting angles of carefully centered reflections corresponded to the cells with dimensions listed in Table 6, where details of the data collection are summarized. The weak reflections ($I < 10\sigma(I)$) were rescanned. Stationary background counts were recorded on each side of the reflection. Three standard reflections were chosen and monitored every 150 reflections.

4.18.2. Data reduction

An empirical absorption correction based on azimuthal scans of several reflections was applied. The

data were corrected for Lorentz and polarization effects. Decay of intensities of three representative reflections was -3.7% for **9**, -3.2% for **10a** and -5.1% for **16**, and thus the linear correction factor was applied to the decay of the observed intensity of the two complexes.

4.18.3. Structure determination and refinement

All calculations were performed using a TEXSAN crystallographic software package from Molecular Structure. Measured nonequivalent reflections with were used for the structure determination. The structures of **10a** and **16** were solved by direct methods (MITHRIL and SHELXS86 [61], respectively) and the structure of **9** by a heavy-atom Patterson method. These were expanded using Fourier techniques. In the final refinement cycle (full-matrix least-squares refinement) of all complexes, hydrogen atom coordinates were included at idealized positions, and were given the same temperature factor as that of the carbon atom to which they were bonded.

Table 6
Crystal data and data collection parameters

	Complex		
	9 · (Me ₂ SO)	10a	16
Formula	C ₂₆ H ₃₆ O ₂ RuS ₄	C ₂₂ H ₂₈ N ₂ RuS ₂	C ₃₁ H ₅₀ N ₂ Cl ₂ As ₂ S ₄ (one dichloromethane as a solvated molecule)
Formula weight	609.88	485.67	924.10
Crystal system	orthorhombic	rhombohedral (hexagonal axes)	monoclinic
Space group	<i>Pna</i> 2 ₁ (#33)	<i>R</i> $\bar{3}$ (<i>h</i>) (#148)	<i>C</i> 2/ <i>c</i> (#15)
<i>a</i> (Å)	8.141(6)	32.595(7)	19.892(4)
<i>b</i> (Å)	16.863(4)		12.038(3)
<i>c</i> (Å)	19.844(7)	10.862(8)	17.107(4)
β (deg)	—		105.52(2)
<i>Z</i>	4	18	4
<i>V</i> (Å ³)	2724(3)	9994(9)	5947(1)
<i>D</i> _{calc} (g cm ⁻³)	1.487	1.452	1.555
Radiation	Mo-K α ($\lambda = 0.71069$ Å)	Mo-K α ($\lambda = 0.71069$ Å)	Mo-K α ($\lambda = 0.71069$ Å)
Crystal size (mm)	0.05 × 0.05 × 0.4	2.00 × 2.00 × 2.00	0.25 × 0.20 × 0.20
Absolute coefficient (cm ⁻¹)	8.79	8.81	11.41
Scan mode	2 θ / ω	ω /2 θ	ω /2 θ
Temperature (°C)	23	23	20
Scan speed (deg min ⁻¹)		8	16
Scan width (deg)		1.42 + 0.35 tan θ	1.21 + 0.30 tan θ
2 θ _{max} (deg)	55.1	55.1	55.0
Data collected	3583	5536	4888
Unique data	3583	5116 (<i>R</i> _{int} = 0.048)	4752 (<i>R</i> _{int} = 0.016)
No. of observations	1920	3955	3919
Criterion of observed	($I > 3\sigma(I)$)	($I > 1.5\sigma(I)$)	($I > 3\sigma(I)$)
No. of variables	298	244	211
<i>R</i>	0.039	0.056	0.045
<i>R</i> _w	0.038	0.071	0.048
GOF	1.17	6.53	6.60
Δ (maximum) (eÅ ⁻³)	0.43	1.52	1.77
Δ (minimum) (eÅ ⁻³)	-0.40	-1.18	-1.45

$$R = \sum ||F_o| - |F_c|| / \sum |F_o|$$

$$R_w = [\sum w(|F_o| - |F_c|)^2 / \sum w F_o^2]^{1/2}, w = 1/\sigma^2(F_o); \text{ function minimized: } \sum w(|F_o| - |F_c|)^2.$$

Acknowledgements

K.M. is grateful for the financial support from the Ministry of Education, Science, Sports and Culture of Japan (nos. 07651057 and 08640711). This work was also supported by the Kurata Foundation.

References

- [1] K. Mashima, A. Mikami, A. Nakamura, *Chem. Lett.* (1992) 1473.
- [2] K. Mashima, H. Kaneyoshi, S. Kaneko, A. Mikami, K. Tani, A. Nakamura, *Organometallics* 16 (1997) 1016.
- [3] M. Kawano, C. Hoshino, K. Matsumoto, *Inorg. Chem.* 31 (1992) 5158.
- [4] K. Matsumoto, H. Uemura, M. Kawano, *Chem. Lett.* (1994) 1215.
- [5] D. Sellmann, J. Küppler, M. Moll, F. Knoch, *Inorg. Chem.* 32 (1993) 960.
- [6] D. Sellmann, P. Kreutzer, G. Huttner, A. Frank, *Z. Naturforsch., B: Anorg. Chem., Org. Chem.* 33 (1978) 1341.
- [7] D. Sellmann, W. Sogliwec, F. Knoch, M. Moll, *Angew. Chem., Int. Ed. Engl.* 28 (1989) 1271.
- [8] S. Kuwata, Y. Mizobe, M. Hidai, *Inorg. Chem.* 33 (1994) 3619.
- [9] K. Mashima, H. Kaneyoshi, S. Kaneko, K. Tani, A. Nakamura, *Chem. Lett.* (1997) 569.
- [10] P. Hofmann, *Angew. Chem., Int. Ed. Engl.* 8 (1977) 536.
- [11] A.R. Siedle, R.A. Newmark, L.H. Pignolet, D.X. Wang, T.A. Albright, *Organometallics* 5 (1986) 38.
- [12] B.K. Campion, R.H. Heyn, T.D. Tilley, *J. Chem. Soc., Chem. Commun.* (1988) 278.
- [13] T.J. Johnson, K. Folting, W.E. Streib, J.D. Martin, J.C. Huffman, S.A. Jackson, O. Eisenstein, K.G. Caulton, *Inorg. Chem.* 34 (1995) 488.
- [14] U. Kölle, J. Kossakowski, *J. Chem. Soc., Chem. Commun.* (1988) 549.
- [15] U. Koelle, J. Kossakowski, *J. Organomet. Chem.* 362 (1989) 383.
- [16] S.D. Loren, B.K. Campion, R.H. Heyn, T.D. Tilley, B.E. Bursten, K.W. Luth, *J. Am. Chem. Soc.* 111 (1989) 4712.
- [17] U. Koelle, C. Rietmann, U. Englert, *J. Organomet. Chem.* 423 (1992) C20.
- [18] A. Takahashi, Y. Mizobe, H. Matsuzaka, S. Dev, M. Hidai, *J. Organomet. Chem.* 456 (1993) 243.
- [19] T.P. Kee, L.Y. Park, J. Robbins, R.R. Schrock, *J. Chem. Soc., Chem. Commun.* (1991) 121.
- [20] R.-M. Catala, D. Cruz-Garriz, P. Sosa, P. Terreros, H. Torrens, A. Hills, D.L. Hughes, R.L. Richards, *J. Organomet. Chem.* 359 (1989) 219.
- [21] K. Mashima, S. Kaneko, K. Tani, *Chem. Lett.* (1997) in press.
- [22] J.J. Garcia, H. Torrens, H. Adams, N.A. Bailey, A. Scacklady, P.M. Maitlis, *J. Chem. Soc., Dalton Trans.* (1993) 1529.
- [23] J.J. Garcia, H. Torrens, H. Adams, N.A. Bailey, P.M. Maitlis, *J. Chem. Soc., Chem. Commun.* (1991) 74.
- [24] R.I. Michelman, R.A. Andersen, R.G. Bergman, *J. Am. Chem. Soc.* 113 (1991) 5100.
- [25] R.I. Michelman, G.E. Ball, R.G. Bergman, R.A. Andersen, *Organometallics* 13 (1994) 869.
- [26] L. Chang, S. Aizawa, M.J. Heeg, E. Deutsch, *Inorg. Chem.* 30 (1991) 4920.
- [27] D. Sellmann, W. Ludwig, G. Huttner, L. Zsolnai, *J. Organomet. Chem.* 294 (1985) 199.
- [28] M.T. Ashby, J.H. Enemark, *J. Am. Chem. Soc.* 108 (1986) 730.
- [29] J.W.E. Cleland, K.M. Barnhart, K. Yamanouchi, D. Collison, F.E. Mabbs, R.B. Ortega, J.H. Enemark, *Inorg. Chem.* (1987) 1017.
- [30] S.B. Choudhury, M.A. Pressler, S.A. Mirza, R.O. Day, M.J. Maroney, *Inorg. Chem.* 33 (1994) 4831.
- [31] H.T. Schacht, R.C. Haltiwanger, M.R. DuBois, *Inorg. Chem.* 31 (1992) 1728.
- [32] H. Matsuzaka, T. Ogino, M. Nishio, M. Hidai, Y. Nishibayashi, S. Uemura, *J. Chem. Soc., Chem. Commun.* (1994) 223.
- [33] W.-F. Liaw, C.-Y. Chuang, W.-Z. Lee, C.-K. Lee, G.-H. Lee, S.-M. Peng, *Inorg. Chem.* 35 (1996) 2530.
- [34] W.-F. Liaw, D.-S. Ou, Y.-S. Li, W.-Z. Lee, C.-Y. Lee, Y.-P. Lee, G.-H. Lee, S.-M. Peng, *Inorg. Chem.* 34 (1995) 3747.
- [35] H. Wang, U. Englert, U. Kölle, *J. Am. Chem. Soc.* 453 (1993) 127.
- [36] E. Alessio, G. Balducci, M. Calligaris, G. Costa, W.M. Attia, G. Mestroni, *Inorg. Chem.* 30 (1991) 609.
- [37] L. Fan, C. Wei, F.I. Aigbirhio, M.L. Turner, O.V. Gusev, L.N. Morozova, D.R.T. Knowles, P.M. Maitlis, *Organometallics* 15 (1996) 98.
- [38] E. Alessio, B. Bolle, B. Milani, G. Mestroni, P. Faleschini, F. Todone, S. Geremia, M. Calligaris, *Inorg. Chem.* 34 (1995) 4722.
- [39] E. Alessio, B. Bolle, B. Milani, G. Mestroni, P. Faleschini, S. Geremia, M. Calligaris, *Inorg. Chem.* 34 (1995) 4716.
- [40] M.A. Bennett, L.Y. Goh, A.C. Willis, *J. Chem. Soc., Chem. Commun.* (1992) 1180.
- [41] M.A. Bennett, L.Y. Goh, A.C. Willis, *J. Am. Chem. Soc.* 118 (1996) 4984.
- [42] T.V. Ashworth, E. Singleton, J.J. Hough, *J. Chem. Soc., Dalton Trans.* (1977) 1809.
- [43] T.V. Ashworth, M.J. Nolte, E. Singleton, *J. Chem. Soc., Dalton Trans.* (1978) 1040.
- [44] F.L. Joslin, M.P. Johnson, J.T. Mague, D.X. Roundhill, *Organometallics* 10 (1991) 2781.
- [45] L. Blum, I.D. Williams, R.R. Schrock, *J. Am. Chem. Soc.* 106 (1984) 8316.
- [46] Z. Nianyong, D. Shaowu, W. Xintao, L. Jiaxi, *Angew. Chem., Int. Ed. Engl.* 31 (1992) 87.
- [47] G.M. Kapteijn, D.M. Grove, W.J.J. Smeets, H. Kooijman, A.L. Spek, G. van Koten, *Inorg. Chem.* 35 (1996) 534.
- [48] M.A. Walters, J.C. Dewan, C. Min, S. Pinto, *Inorg. Chem.* 30 (1991) 2656.
- [49] J. Huang, R.L. Ostrander, A.L. Rheingold, Y. Leung, M.A. Walters, *J. Am. Chem. Soc.* 116 (1994) 6769.
- [50] N. Ueyama, T. Okamura, A. Nakamura, *J. Am. Chem. Soc.* 114 (1992) 8129.
- [51] J. Amarasekera, T.B. Rauchfuss, *Inorg. Chem.* 28 (1989) 3875.
- [52] D. Sellmann, I. Barth, M. Moll, *Inorg. Chem.* 29 (1990) 176.
- [53] D. Sellmann, R. Ruf, F. Knoch, M. Moll, *Inorg. Chem.* 34 (1995) 4745.
- [54] P.M. Treichel, L.D. Rosenhein, M.D. Schmidt, *Inorg. Chem.* 22 (1983) 3960.
- [55] P.M. Treichel, L.D. Rosenhein, *Inorg. Chem.* 23 (1984) 4018.
- [56] A. Shaver, M. El-khateeb, A.-M. Lebus, *Inorg. Chem.* 34 (1995) 3841.
- [57] M.A. Bennett, T.-N. Huang, T.W. Watheson, A.K. Smith, *Inorg. Synth.* 21 (1982) 74.
- [58] I. Kuwajima, M. Shimizu, H. Urabe, *J. Org. Chem.* 47 (1982) 837.
- [59] M. Akiba, M.V. Lakshminantham, K.-Y. Jen, M.P. Cava, *J. Org. Chem.* 49 (1984) 4819.
- [60] K. Mashima, K. Kusano, Y. Matsumura, N. Sato, K. Nozaki, H. Kumobayashi, Y. Hori, T. Ishizaki, S. Akutagawa, H. Takaya, *J. Org. Chem.* 59 (1994) 3064.
- [61] G.M. Sheldrick, *Crystallographic computing*, in: G.M. Sheldrick, C. Krüger, R. Goddard (Eds.), *Crystallographic Computing* 3, Oxford Univ. Press, Oxford, 1985, p. 179.